Pure appl. geophys. 162 (2005) 2071–2093
0033–4553/05/112071–23
DOI 10.1007/s00024-005-2705-8

Pure and Applied Geophysics

Application of Analytical Modeling to the Far-field Investigation of Tsunami and Oceanic Rayleigh Waves from the 1998 Papua New Guinea Earthquake

TATYANA NOVIKOVA,[1] BOR-SHOUH HUANG,[1] and KUO-LIANG WEN[2]

Abstract—We analyze far-field Rayleigh and tsunami waves generated by the 1998 Papua New Guinea (PNG) earthquake. Using the normal mode theory and Thomson-Haskell matrix formalism we calculate synthetic mareograms of oceanic surface waves excited by finite-dimensional line source and propagated in a flat, multilayered oceanic structure. Assuming that the source of destructive sea waves was the main shock of the PNG event and based on the expression for seismic wave displacement in the far-field zone, we compute the energy of the seismic and tsunami waves and the E_z/E_{ts} ratio. The results of our modeling are generally consistent with those obtained empirically for events with magnitude 7. Also, treating the results of a submarine slide as a single solitary wave and using the theoretical arguments of STRIEM and MILOH (1976) we estimate the energy of the tsunami induced by a landslide. The difference between the energy of the seismic tsunami and of the aseismic one is about one order of magnitude.

The results of our theoretical modeling show that surface sea waves in the far-field zone account well for seismic origin, although additional tsunami energy from a landslide source could be required to explain the local massive tsunami in the Sissano Lagoon.

Key words: Tsunami, Rayleigh waves, far-field zone, seismic origin, point and distributed source, submarine slump, energy estimation.

1. Introduction

Seismicity and Historical Tsunamis along the North Coast of New Guinea

Since the onset of our understanding of tectonic evolution history, the region of the southwest Pacific in the vicinity of the New Guinea landmass has widely been regarded as one of the most tectonically complex areas of the world. The complicated convergent Australian-Pacific plate boundary which results in a high frequency of earthquakes makes Papua New Guinea (PNG) and its environs a particularly important region for consideration from a tectonic point of view. Present GPS observations (PUNTODEWO *et al.*, 1994) show that the oblique convergence between

[1]Institute of Earth Sciences, Academia Sinica, Taiwan. E-mail: tatyana@egelados.gein.noa.gr
[2]Institute of Applied Geology, NCU, USA

the north Bismark microplate and the Pacific plate is highly partitioned between thrusting at the New Guinea trench and at the inland thrust belts, and strike-slip at the inland faults. Estimating plate tectonic motions in PNG from GPS data, TREGONING *et al.* (1998) have noted that up to four minor plates (South and North Bismarck Plates, Solomon Sea Plate, Woodlark Plate) may be trapped in the collision in response to the convergence of the two major plates, namely the Australian and Pacific. On the other hand, PNG and its surrounding areas also comprise a region of both active and dormant volcanoes and of intense and frequent earthquake activity at all depths. Analyzing the seismic activity, focal mechanisms and earthquake epicenter distribution in western New Guinea, SENO and KAPLAN (1988) have found that near the junction of the transform fault in the Bismarck Sea with the New Guinea coast, both thrust-type and strike-slip-type mechanisms can occur. Thrust-type mechanisms with additional strike-slip components may represent underthrusting of the Bismarck plate beneath the New Guinea landmass. The strike-slip events show left-lateral motion between the north and south Bismarck plates.

The location of Papua New Guinea within one of the most tectonically complex regions in the world makes this area highly vulnerable to tsunamis. Unfortunately, very few historical tsunamis have been documented in this area. Possibly though one of the strongest tsunamis was excited by the earthquake of magnitude 8.0 (M_s) in 1873 which effected the northeastern coast of the island (SOLOVIEV and GO, 1974). The lack of quantitative data for this event makes further analysis impossible. On December 15, 1907, magnitude 7 an earthquake generated a tsunami which hit the area west of Aitape. On September 20, 1935 near the northern shoreline in almost the same area as the 1998 event, an earthquake with magnitude 7.9 struck creating seismic sea waves. However, no tsunami intensity values or run-up heights are available in the database. To the east of the present (1998) event, 4-meter waves were observed after a magnitude 7.0 earthquake on October 31, 1970 near Madang. The 1998 PNG earthquake occurred as a result of high seismic activity at the plate boundary between the north Bismarck microplate (its existence and location to the north of PNG was proposed by JOHNSON and MOLNAR, 1972) and the Australian plate. This boundary lies along the New Guinea Trench which accommodated active southward subduction, according to the seismic profile near the 1998 earthquake epicenter, as presented by HAMILTON (1979) (Fig. 1). In conjunction with this earthquake a massive tsunami was generated with maximum heights of 10 m and in some case 15 m concentrated on the 30-km coastal area of Papua New Guinea.

Attempts at Numerical Simulation of the PNG Tsunami

The main shock of the PNG event was originally considered to be the immediate origin of the massive tsunami wave, which struck the Sissano Lagoon with a maximum run-up of 15 m. From this point of view, numerous attempts have been made to answer two related questions. For one, what was the reason for such

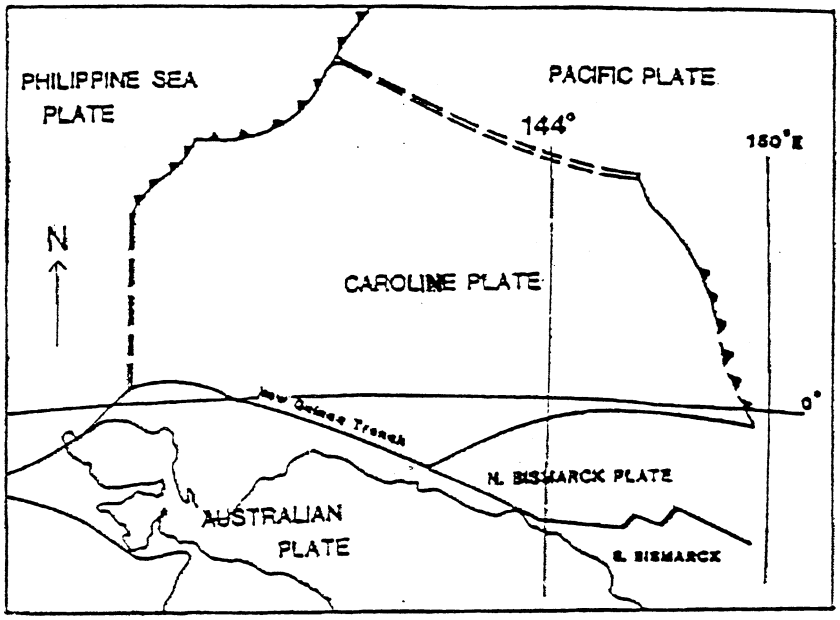

Figure 1
Major plates in the southwest Pacific in the vicinity of New Guinea (after Hamilton, 1979).

tsunami concentration in the Sissano region? Secondly, is an additional source such as a sediment slump necessary to explain tsunami amplitudes in the near and far-field zones?

Based on a near-field tsunami numerical simulation MATSUYAMA *et al.* (1999) have shown that a factor responsible for the tsunami concentration in the Sissano region was the bathymetry of the area. Their 2-D numerical model includes both the attenuating effects of geometric spreading and the focusing effects of lateral changes in bathymetry off the Sissano Lagoon. A steep reverse fault has been suggested as the tsunamigenic source. Using a mid-slope source location for the earthquake, the authors have predicted a maximum run-up of 8 m. They also have performed a simulation for a low-angle reverse fault to evaluate it as a probable tsunami source. However, the numerical experiment has demonstrated that this seismic source is capable of generating a tsunami when accompanied by a large underwater landslide.

Another near-field study of locally destructive tsunamis, however, provides evidence favoring an aseismic origin. HEINRICH *et al.* (2001) have carried out a finite-difference landslide and tsunami simulation in the near-field zone based on a shallow-water approximation. In their model, water waves were generated by sea-bottom displacements induced by a landslide. The landslide was treated as a flow of a homogeneous gravity-driven continuum governed by a rheological law. 2-D simulation results confirmed that the PNG tsunami was likely caused by a deep

(with its top located at a water depth of 550 m) and large (4 km^3 volume) submarine landslide sliding with a Coulomb-type friction law over a 5-km distance. This scenario is analogous to other historical events, e.g., 1994 in Skagway Harbor in Alaska, and 1929 in Grand Banks. In the case of the Grand Banks event, an earthquake that occurred near the continental margin triggered a submarine landslide, which consequently caused a tsunami.

For teleseismic tsunami modeling, TANIOKA (1999) has adopted the linear Boussinesq equations with Coriolis forcing and solved them numerically using a finite-difference scheme. His results favor a steeply dipping reverse fault as a source and the occurrence of the PNG earthquake within a small accreationary prism near the New Guinea Trench.

According to the analysis of seismic data for the PNG event, the difference between the tsunami magnitude (M_t), as determined from tide-gauge data at long distance, and the one of the earthquake (M_s), was about 0.4. ABE (1979) quantified earthquakes accompanied by tsunamis with a discrepancy in terms of the surface wave magnitude and tsunami magnitude scales of about 0.5 as the class of tsunami earthquakes (KANAMORI, 1972). Tsunami earthquakes have common features (SATAKE and TANIOKA, 1999). First the coseismic slip is concentrated on a narrow, shallow region near the trench axis. Secondly, this region is located beneath an accretionary wedge and it is limited on the order of 10 km extent below the ocean bottom.

From the first point of view, the analysis of seismic data together with the geomorphology of the epicentral region favors the PNG event being classified as the tsunami earthquake type. Additionally, with regard to tsunami earthquake classification, NEWMAN and OKAL (1998) have identified the parameter of "slowness" using the ratio between high-frequency energy E and low-frequency seismic moment M_0. For typical tsunami earthquakes such as the 1992 Nicaragua event, the value of the slowness parameter is equal to −6.30, and in fact for the 1994 Java event it was estimated as −6.01. Following Newman and Okal's procedure KAWATA *et al.* (1999) and later SYNOLAKIS *et al.* (2002) have estimated this parameter for the PNG main shock event (= −5.67) and the aftershock (= −4.67) and finally concluded that the PNG earthquake was not the case of slow released energy. The possibility of slow rupture during the PNG event has also been discussed by KIKUCHI *et al.* (1999). Based on the teleseismic body P- and S-wave record analysis and the empirical relations between the source duration τ and seismic moment M_0, the authors estimated the M_0/τ^3 ratio and found that it was well within the range for ordinary earthquakes. Thus, their analysis has also precluded the notion of slow rupture as the probable origin of the PNG destructive seismic sea waves. As concerns a tsunami source they have suggested a high-angle dip-slip fault. However, their research does not exclude the possibility of an additional source such as an aseismic submarine landslide. This possibility was also not rejected in the study of GEIST (2000). Using the 1-D analytical

N-wave run-up law for a deep water source, he has predicted run-ups of between 5 and 9 m, which consequently would indicate that a significant tsunami would have been generated in the case of the PNG earthquake. He has, however, emphasized that the PNG event is likely neither a result of a pure seismic source nor due to a pure slump source. His conclusion, therefore, was that the earthquake origin of the PNG tsunami is consistent with some Pacific tide gauge records (in particular in Japan), although additional tsunami energy from a landslide source might be necessary to explain local tsunami amplitudes in the Sissano Lagoon.

Submarine Slump as a Probable Tsunami Origin of the PNG Event

There are differences between tsunamis generated by a coseismic seafloor displacement (class "a") and those generated by a submarine sediment slump (class "b"). The first is with respect to wavelengths and periods. Tsunamis belonging to class "a" are usually characterized by wavelengths of 20 to 100 km and periods of between 20 and 80 min, whereas landslide-generated tsunamis have much shorter wavelengths of about 1–10 km and periods of 1 to 5 min. The second distinction between the two classes of tsunami concerns the influence of frequency dispersion during wave propagation. It is negligible for tectonically-generated tsunamis (since its amplitude decays slowly), while slump-generated sea waves attenuate quickly due to the frequency dispersion of deep water.

Underwater landslides are a common source of small-scale tsunamis in coastal areas. The most common reason for a submarine slide is an oversteepening of a slope or liquefaction of sediment. The slides can flow some hundreds of meters, even kilometers, over gentle slopes (as low as 1°–2°), and transport large amounts of soil and sand. In order for a slump to generate a tsunami with heights of 10 to 15 m, it must be huge (tens of kilometers wide and hundreds of meters thick). Nevertheless, there have been several instances of large water waves which were generated by underwater landslides. Among them are such events as the 1929 Grand Banks (HASEGAWA and KANAMORI, 1987), 1956 Amorgos, Greece (AMBRASEYS, 1960) and 1975 Kalapana, Hawaii (EISSLER and KANAMORI, 1987).

In the case of the PNG event slump features have been identified. Using seismic reflection data, SWEET *et al.* (1999) have precisely mapped their presence, structure and geometry. The investigation of the seafloor morphology reveals the appearance of an amphitheater as a result of slumping. Futher, it was established by marine surveys that the submarine slump was composed of cohesive sediments and bedrock, sliding a few kilometers without large disturbances. In particular TAPPIN *et al.* (1999, 2000) have well documented the following: "The southern (headwall) slope of the amphitheater itself shows collapse features in both bedrock and cohesive sediment. At the foot of the headwall scarp is fresh fissuring in cohesive sediment. The southern margin of the upraised block shows recent faulting, talus debris slopes, and headwall collapse." Based on these findings'

data, the landslide volume covers an area of approximately 5 km by 3 km, with a maximum thickness of 450 m. The volume is located at water depths between 550 and 1500 m on a 15° slope.

Although this evidence supports the hypothesis of the occurrence of a slide at some point in the past, there is no particular evidence to suggest exactly when it happened. Not to be ignored however is that MATSUYAMA *et al.* (1999), in analyzing the epicenteral area of the PNG earthquake, have noted that the shelf along the north coast of Papua New Guinea is narrow, and fluvial sediments continually escape to the continental slope and beyond. The high sediment flux offshore may in fact allow a large thickness of sediment to accumulate. Thick sediment combined with the steep, active margin setting make this region particularly susceptible to submarine landslides. Even so, from these authors' point of view there is no particular evidence for such a well-defined large slump that would have created a tsunami with a maximum run-up of 10–15 m in this area. In keeping with this, IWABUCHI (2000) has shown that no recent turbidities can be recognized from piston core samples on the lobe of the presumed landslide and that the geomorphological features of this landslide are not recent.

SYNOLAKIS *et al.* (2002) have presented undoubtedly one of the most interesting and complete analysis in favor of aseismic origin of PNG tsunami. Analyzing the tsunami amplitudes and timing, based on available bathymetric and seismic images, the authors have strongly supported the scenario of the generation of the PNG tsunami by a large underwater slump at 09.02 GMT. The delay of 13 min between the main shock and the initiation of the slump they have attributed to the nucleation of failure in the sedimentary mass. According to their final conclusion there is no model of seismic dislocation for the generation of the tsunami which would be compatible with the full set of available seismological observations, with morphological and structural observations from the shipboard surveys, and with the timing of the wave at the shore, as reconstructed from survivor interviews.

In summarizing the facts described above, it is reasonable for us to conclude that an exact mechanism for the generation of destructive PNG tsunamis remains debatable. Evidence based solely on eyewitness accounts observation can be taken as favoring the slump tsunami generation theory. Of particular interest too is the delay of about 10 min between the main shock and the tsunami arrival at Sissano. The coast was effected about 20 min after the main shock, but in fact, the travel time of seismic water waves is only about 10 min from a source located 20 km offshore Sissano. Thus, a tsunami from the area at the foot of the slump would probably take 10 minutes to strike the nearest shore zone. In the case of seismic tsunami generation a fault would be expected to create a wave almost immediately. However, it is interesting to note there is another explanation for tsunami arrival time at Sissano proposed by RIPPER and LETZ (1999). Employing the survey's field reports and seismograph data, they tracked the PNG earthquake

and considered it was a doublet of magnitude 7 and the Sissano tsunami followed the second main earthquake within 5–10 minutes. Therefore, the tsunami arrival time at Sissano can be explained by both fault and slump-generated mechanisms.

In this paper we present an analytical model to study surface sea waves (Rayleigh and tsunami) generated by an underwater earthquake. The effect of different source scenarios on seismic sea waves is one focus of this study. The other deals with energy estimation of both a fault- and of a slump-generated tsunami. Surface-sea waves propagating in multilayered oceanic media are treated using the normal mode theory and THOMSON (1950) and HASKELL (1953) matrix formalism.

2. Statement of the Problem

The statement of the problem is similar to that described in NOVIKOVA *et al.* (2002). Here, therefore, we only briefly review the main points of the theory. The model used to study tsunami and Rayleigh wave far-field propagation assumes two homogeneous, isotropic layers overlying a homogeneous half-space. A superficial layer of uniform thickness H is assumed to be a compressible nonviscid liquid. Between the liquid and the half-space, there is a layer of hard sediments.

In such a system the equations of motion are written in the linear theory approximation (POD''YAPOL'SKY, 1968, 1970; GUSIAKOV, 1975):

$$\lambda_0 \nabla \text{ div } \mathbf{u} - \rho_0 g \hat{\mathbf{e}}_z \text{ div } \mathbf{u} = \rho_0 \frac{\partial^2 \mathbf{u}}{\partial t^2} \quad \text{at } 0 < z < H, \tag{1}$$

and

$$(\lambda_m + 2\mu_m) \nabla \text{ div } \mathbf{u} - \mu_m \text{curl}(\text{curl } \mathbf{u}) = \rho_m \frac{\partial^2 \mathbf{u}}{\partial t^2} \quad \text{at } z > H. \tag{2}$$

Here c_f is the velocity of the acoustic wave in the liquid layer; λ_0, λ_m and μ_m and ρ_0, ρ_m are the Lamé parameters and densities of the liquid and solid medium, respectively; $\mathbf{u}_i = (U_i, 0, W_i)$ is the displacement vector ($i = 0$ for the liquid layer, $i = 1$ for the sedimentary layer and $i = 2$ for the half-space), g is gravity; ω is the angular frequency; $\hat{\mathbf{e}}_z$ is the unit normal vector and z is the depth from the free surface (positive downwards).

The boundary conditions to be satisfied are as follows: The vanishing of pressure at the surface of the liquid layer; the continuity of normal component displacement and stress and the vanishing of shear stress at the liquid-solid interface; the continuity of two displacement and stress components at the solid-solid interface; and the vanishing of the displacement at $z \rightarrow \infty$.

3. Solution

We seek the solution to the motion equations in the form of the plane wave propagating in the horizontal direction of increasing x with frequency ω and phase velocity c and the amplitude decreasing exponentially in the positive downward z direction in the half-space:

$$\mathbf{u}_i(x,z,\omega,t) = \mathbf{v}_i(z,\omega)\exp[i\omega(t-x/c)]. \tag{3}$$

With (3) substituted into equations (1) and (2) and the boundary condition at $z \to \infty$ introduced, the wave amplitudes as a function of depth yield:

$$U_0(z,\omega) = \frac{ic_f^2}{\omega c}\left[-A_0\exp\left(-\eta_{02}z/c_f\right) + B_0\exp\left(-\eta_{01}z/c_f\right)\right], \tag{4}$$

and

$$W_0(z,\omega) = -\frac{c_f}{\omega^2}\left[-\eta_{01}A_0\exp\left(-\eta_{02}z/c_f\right) + \eta_{02}B_0\exp\left(-\eta_{01}z/c_f\right)\right] \tag{5}$$

for the liquid layer, where:

$$\eta_{01} = -\omega\gamma - g/2c_f, \tag{6}$$

and

$$\eta_{02} = \omega\gamma - g/2c_f \tag{7}$$

$$\gamma^2 = \frac{c_f^2}{c} - 1 + \frac{g^2}{4c_f^2\omega^2}, \tag{8}$$

for the sedimentary layers:

$$\begin{aligned} U_1(z,\omega) = {} & \frac{ia_1^2}{\omega c}\left(C_1\exp(-\omega\alpha_1 z/a_1) + D_1\exp(\omega\alpha_1 z/a_1)\right) \\ & - \frac{i\beta_1 b_1}{\omega}\left(E_1\exp(-\omega\beta_1 z/b_1) + F_1\exp(\omega\beta_1 z/b_1)\right) \end{aligned} \tag{9}$$

$$\begin{aligned} W_1(z,\omega) = {} & \frac{\alpha_1 a_1}{\omega}\left(C_1\exp(-\omega\alpha_1 z/a_1) + D_1\exp(\omega\alpha_1 z/a_1)\right) \\ & - \frac{b_1^2}{\omega c}\left(E_1\exp(-\omega\beta_1 z/b_1) + F_1\exp(\omega\beta_1 z/b_1)\right), \end{aligned} \tag{10}$$

and for the half-space,

$$U_2(z,\omega) = \frac{ia_2^2}{\omega c}C_2\exp(-\omega\alpha_2(z-H)/a_2) - \frac{ib_2\beta_2}{\omega}E_2\exp(-\omega\beta_2(z-H)/b_2), \tag{11}$$

and

$$W_2(z,\omega) = \frac{a_2\alpha_2}{\omega}C_2\exp(-\omega\alpha_2(z-H)/a_2) - \frac{b_2^2}{\omega c}E_2\exp(-\omega\beta_2(z-H)/b_2), \tag{12}$$

where

$$\alpha_{1,2}^2 = \begin{cases} i\left(1 - a_{1,2}^2/c^2\right)^{1/2} & \text{if} \quad c > a_{1,2} \\ \left(a_{1,2}^2/c^2 - 1\right)^{1/2} & \text{if} \quad c < a_{1,2} \end{cases} \quad (a = \text{compressional wave velocity}) \tag{13}$$

$$\beta_{1,2}^2 = \begin{cases} i\left(1 - b_{1,2}^2/c^2\right)^{1/2} & \text{if} \quad c > b_{1,2} \\ \left(b_{1,2}^2/c^2 - 1\right)^{1/2} & \text{if} \quad c < b_{1,2} \end{cases} \quad (b = \text{shear-wave velocity}). \tag{14}$$

The system of boundary conditions comprises a number of homogeneous equations with unknown coefficients. To determine these later, the periodic equation has to be solved. The Thomson-Haskell technique is used here to construct the dispersion function. The idea of the method is the creation of the layer matrices that relate the components of motion at one interface in a layered structure to those at the next. The product of these layer matrices then relates the components of motion at the deepest interface to those at the free surface, and in the final stage, this layer-matrix product is then used to construct the dispersion function.

In the final form the dispersion equation can be written as follows (HASKELL, 1953):

$$\Delta(\omega, c) = H_{11}T_{12} - H_{12}T_{11} = 0. \tag{15}$$

The components of the matrices H and T as well as the details of the solution of the dispersion equation are given in NOVIKOVA *et al.* (2002).

4. Tsunami and Rayleigh Waves from Point and Distributed Source

To derive the expression for the displacement of a stationary surface wave excited by a point source in the homogeneous half-space, we follow the theory of surface waves in the vertically inhomogeneous media as developed by LEVSHIN (1978), KEILIS-BOROK (1989). It is based on the expansion of the solution into eigenfunctions of the boundary problem. In the context of this approach, the spectrum of displacement in an interference wave (Rayleigh and Love) can be expressed as a product of four factors. The first is the complex constant, while the second describes the effect of geometric divergence of the energy flow on wave propagation. The third term depends on the depth of the receiver, and the final one depends on the source parameters, i.e., on the depth, focal mechanism and the radiation spectrum.

In the far-field approximation of this theory, the expression of displacement in a surface wave generated by the point source at the depth h in the solid earth is the following:

$$\mathbf{u}(r,\varphi,\omega,t) = \frac{\exp(-i\pi/4)}{\sqrt{8\pi}} \frac{\exp(i\omega(t-r/c))}{\sqrt{\omega r/c}} \frac{\mathbf{U}(z,\omega)}{\sqrt{cu_0 I_0}} \frac{Q_\chi(h,\varphi,\omega)}{\sqrt{cu_0 I_0}}, \tag{16}$$

where $\mathbf{U}(z,\omega) = U(z,\omega)\mathbf{e}_r + W(z,\omega)\mathbf{e}_z$, $Q_\chi(h,\varphi,\omega) = m_{rs}(\omega)B_{rs}(h,\varphi,\omega)$ is the excitation function; $m_{rs}(\omega)$ is the spectrum of the seismic moment tensor; and $B_{rs}(h,\varphi,\omega)$ is a tensor which can be expressed via the eigenfunctions $U(z,\omega)$ and $W(z,\omega)$ and their derivatives and which depend on the axis orientation of the source (φ); $I_0 = \int \rho(z)\left[U^2(z,\omega) + W^2(z,\omega)\right] dz$ represents the energy; u_0 is the group velocity. For a dipolar point source with arbitrary elements BEN-MENAHEM and HARKRIDER (1964) have given the expression for the term which represents the azimuthal dependence of the excitation factor:

$$\chi(\theta,h) = d_0 + i(d_1 \sin\theta + d_2 \cos\theta) + d_3 \sin 2\theta + d_4 \cos 2\theta, \tag{17}$$

where d_i are

$$d_0 = \frac{1}{2_1} \sin\lambda \sin 2\delta B(h); \quad d_1 = -\sin\lambda \cos 2\delta C(h); \quad d_2 = -\cos\lambda \cos\delta C(h);$$
$$d_3 = \cos\lambda \sin\delta A(h); \quad d_4 = -\frac{1}{2}\sin\lambda \sin 2\delta A(h),$$

where h is the source depth, θ is the angle between the strike of the fault and the direction epicenter-station measured counter-clockwise, and δ, λ are the dip and rake angles, respectively. Depth-dependent factors through the eigenfunctions are as follows:

$$A(h) = -i\frac{\omega}{c}U(h);$$
$$B(h) = -i\frac{\omega}{c}U(h)\left[3 - 4\frac{b^2(h)}{a^2(h)}\right] - 2\left[\left.\frac{\partial W}{\partial z}\right|_h - i\frac{\omega}{c}U(h)\left(1 - 2\frac{b^2(h)}{a^2(h)}\right)\right];$$
$$C(h) = \left.\frac{\partial U}{\partial z}\right|_h - i\frac{\omega}{c}W(h), \tag{18}$$

where a and b are the P- and S-wave velocities.

To estimate the source radiation function, some value of the seismic moment M_0 and its spectrum $F(\omega)$ must be assumed. We assume values of the radiation function up to the factor M_0 and for the azimuth along which seismic radiation is maximal. Thus,

$$F(\omega) = \frac{1}{i\omega(i\omega\tau_0 + 1)}, \tag{19}$$

where τ_0 is the rise time.

In the present study we consider, using the above mentioned mathematical derivations for the point source, a finite-dimensional line source (rupture extending

over a long fault). This can be modeled by a set of point sources, uniformly distributed along the fault and moving along it at a constant velocity. For calculations we ignore the two-dimensionality of the fault.

When rupture propagates in an azimuth different from the strike of the fault, there is an additional influence of the effect on the excitation coefficients of the variation in depth introduced by the up- or down-dip component of the rupture propagation vector. Taking it into account, we can possibly see changes in the directivity factor for two conjugate faults.

With the relation between the moment tensor (M) and the moment density tensor (m) in the form

$$M_{pq} = \int_L m_{pq}\, dL \tag{20}$$

the normalized excitation function in the case of the finite-dimensional line source becomes:

$$\frac{\widetilde{Q}_\chi(h,\omega,\varphi)}{\sqrt{cu_0 I_0}} = \int_0^{L_0} m(\omega,L)\exp\left[-i\omega L\left(\frac{1}{V}\mp\frac{\cos\alpha}{c}\right)\right]\frac{Q_\chi\left(h^1,\omega,\varphi\right)}{\sqrt{cu_0 I_0}}\, dL, \tag{21}$$

where $h^1_{L_0} = h_0 - L\sin\phi$ is the change of the depth with rupture propagation; moment density $\int_0 m(\omega,L)\, dL = M_0(\omega)$; L_0 is the fault length; V is the velocity of the rupture propagation; c is the phase velocity; ϕ is the angle between the rupture and its horizontal projection (itself a function of the dip of the fault and the difference of horizontal azimuth between rupture and fault strike; $L\left(\frac{1}{V}\mp\frac{\cos\alpha}{c}\right)$ is the rupture time; α is the azimuth of the station with respect to the fault strike. This angle should be calculated taking into account that rupture propagates in an azimuth different from the strike of the fault.

Given that the earthquake rupture velocity V is typically about 80% ± 10% of the shear velocity, based on the standard definitions of seismic moment along with empirical observations (BILEK and LAY, 1999), formula (21) can be rewritten in the following form:

$$\frac{\widetilde{Q}_\chi(h,\omega,\varphi)}{\sqrt{cu_0 I_0}} = \int_0^{L_0} m(\omega,L)\exp\left[-i\omega L\left(\frac{1}{0.8\sqrt{\mu/\rho}}\mp\frac{\cos\alpha}{c}\right)\right]\frac{Q_\chi\left(h^1,\omega,\varphi\right)}{\sqrt{cu_0 I_0}}\, dL, \tag{22}$$

where μ and ρ are the rigidity and rock density, respectively. Since the PNG earthquake was not the case of a slow rupturing event (SYNOLAKIS *et al.* 2002), the formula $V_{(\text{rupture})} = 0.8\, V_s$ can be justly used for calculations.

5. Energy of Surface Wave

The energy of a tsunami wave is estimated as the total energy flux through a cylindrical surface. Taking into account the Parseval theorem considered, it can be written in the frequency domain as:

$$E = \frac{1}{2\pi} \iint\limits_{S} r\, d\varphi\, dz \int\limits_{0}^{\infty} \frac{\rho\omega^2 |u(r,\varphi,\omega)|^2}{2} u_0\, d\omega, \tag{23}$$

where u_0 — is the group velocity; r—is the horizontal distance from the source; φ —is the azimuth angle; and s —is the surface of half-infinite cylinder with radius r and axis $z = 0$ so that $ds = rd\varphi\, dz$.

With (16) substituted into (23), one reasons that the expression for the energy of surface waves is obtained as follows:

$$E = \frac{1}{16\pi} \int\limits_{0}^{\infty} \frac{\omega \hat{Q}^2(h,\omega)}{cu_0 I_0}\, d\omega, \tag{24}$$

where

$$\overset{\Lambda}{Q}(h,\omega) = \frac{1}{2\pi} \int\limits_{0}^{2\pi} Q(h,\omega,\varphi)\, d\varphi \text{ and } I_0 = \int \rho(z) \left[U(z,\omega)^2 + W(z,\omega)^2 \right] dz.$$

Since the characteristic rise time in the source τ_0, which depends on M_0, appears in the integrand in the formula for tsunami energy, the latter will also depend on M_0; however, it will not be proportional to the square of seismic moment.

5a. Empirical Approach to Tsunami Energy Estimation

Tsunami energy depends not only on the magnitude of an earthquake but also on the conditions of tsunami generation and propagation. Focal depth, water depth at the epicenter, rupture velocity and amount of vertical displacement of the sea bottom may all effect the generation of tsunamis. Well known are numerous examples of tsunamigenic earthquakes that have produced substantial slip such as Sanriku, 1933 (vertical displacement $a_m = 6.5$ m), Sanriku, 1936 (vertical displacement $a_m = 7.1$ m), Tonankai, 1944 (vertical displacement $a_m = 10.0$ m), and Kamchatka, 1952 (vertical displacement 10.7 m).

Varieties of empirical methods were proposed for tsunami energy estimation. They were classified by KAJIURA (1981) as follows: Relative energy method which is based on the qualitative definition of IMAMURA's (1942) tsunami magnitude; energy flux method assuming the isotropic character of radiation energy from a point source (TAKAHASI, 1951); reverberation method; spectral inversion method assuming the

axial symmetry of initial disturbance; potential energy method; numerical inversion method on the basis of shallow water equations solution.

On the basis of a simple kinematic similarity model of the earthquake fault, KAJIURA (1981) proposed an advanced expression for tsunami energy estimation. According to his analysis, the relation between the tsunami energy E_{ts} and parameters $(M_w, \delta, \lambda, h^*)$ of the earthquake fault is

$$E_{ts} = \frac{1}{2}\rho g\left(\alpha^{2/3}/\mu^2\right)M_0^{4/3}F(\delta, \lambda, h, r), \tag{25}$$

where ρ is the density of water; α is the constant of proportionality, which appears to vary by a factor of 3 depending on the tectonic setting of the region in which the earthquake takes place ($\alpha \approx 1.23 \times 10^7$ dyne.cm^{-2} for interplate earthquakes and $\alpha \approx 3 \times 10^7$ dyne.cm^{-2} for the intraplate events); μ is the rigidity of the media; M_0 is the earthquake moment and $F(\delta, \lambda, h, r)$ is a function of fault parameters, defined as

$$F(\delta, \lambda, h, r) = \int\limits_{s'/s} z_*(\delta, \lambda, h, r)^2\, dS_*, \tag{26}$$

where the bottom displacement scaling in terms of the dimensions of a plane fault is $z_* = z/D$, $dS_* = dS/S$, $h = H/L$, $r = W/L$. Allowing for the relationship $M_w = (\log M_0 - 16.1)/1.5$, tsunami energy in relation to parameters of the earthquake fault is:

$$\log E_{ts} = 2M_w + \log F + 5.5 \text{ (for interplate earthquakes).} \tag{27}$$

5b. Energy of a Tsunami Wave Induced by a Submarine Slump

An empirical method has been proposed by MILOH and STRIEM (1978) for estimating the energy of waves induced by a submarine slide. According to their analysis wave energy is uniformly distributed over a finite width of the slide, and during the sliding process the potential energy of the slide which is

$$E_p = gLWh(\rho_s - \rho_w)(D_0 - D_s), \tag{28}$$

is partially (fraction is 0.01) converted into the surface wave energy and into the kinetic energy of the mudflow and viscous energy dissipation. The wave generated by a slide is characterized as a solitary wave. Equation (28) assumes that the slump is cohesive and is applicable for the PNG event. According to marine surveys (TAPPIN *et al.*, 1999), a submarine slump that is likely caused the 1998 PNG tsunami was composed of cohesive sediments and bedrock.

In the formula for the potential energy of the slide (E_p) the following characteristics are used: L—is the length of the slide; W— is the width of the slide; h— is the average thickness of the slide material; ρ_s and ρ_w are the densities of the sea bottom material and sea water; D_s and D_0 are the water depths at the ends of the slide and slope, respectively.

Table 1

Parameters of the model

Liquid layer	c_f = 1.45 km/s; ρ_1 = 1.0 g/cm^3; H = 4.0 km
Hard sedimentary layer	V_p = 6.5 km/s; V_s = 3.74 km/s; ρ_2 = 2.87 g/cm^3; h_2 = 18.0 km
Elastic half-space	V_p = 7.8 km/s; V_s = 4.4 km/s; ρ_3 = 3.3 g/cm^3.

6. Results of Numerical Modeling

We simulate far-field tsunami and Rayleigh wave propagation, using a layered Ocean-Earth model with the parameters given in Table 1. The choice of elastic constants is quite similar to the model for teleseismic data analysis, applied by KIKUCHI *et al.* (1999).

Assuming, initially, a seismic origin of the PNG tsunami, as mentioned above, we carry out calculations for different source scenarios including the mechanism of the largest aftershock. Source mechanism parameters are summarized in Table 2. According to KIKUCHI *et al.* (1999) estimations, up-dip rupture propagation is required only for shallow plane, and strong down-dip propagation on the steep one. Therefore, in our calculations we assumed up-dip rupture propagation in case of shallow-dipping source (second scenario), and rupture with down-dip direction for the steep faults (first and third scenario). Following SYNOLAKIS *et al.* (2002), we have assumed the rupture with velocity 2.99 km/s and azimuth $\phi_R = 85^\circ$ propagates from initial hypocentral depth at 17.7 km, and slight up-dip propagation (in the case of the second scenario) results in a final depth of 4.8 km.

Modeling the PNG tsunami MATSUYAMA *et al.* (1999) have proven that the two earthquake solutions: The high angle reverse fault indicative of an inner plate earthquake and the low angle fault indicative of a plate boundary earthquake are equally capable of tsunami generation. The latter, however, produces a vertical seabed displacement three times smaller than the former. Our simulations predict similar behavior. Figure 2 displays the tsunami and Rayleigh wave excitation functions for different geometries of the extended seismic source (the forth multiplier of (16)). It is evident that the amplitude of the tsunami excitation maximum in the case of a high dip angle faults (curves 1, 3) is more than one order of magnitude

Table 2

Source parameters used in modeling

	First scenario—high-angle main shock (1)	
Fault strike (deg.)	Dip (deg.)	Rake (deg.) and references
301	86	91 (KIKUCHI *et al.*, 1999)
	Second scenario—low-angle main shock (2)	
146	19	127 (DZIEWONSKI *et al.*, 1999)
	Third scenario—high-angle aftershock (3)	
111	75	−105 (KIKUCHI *et al.*, 1999)

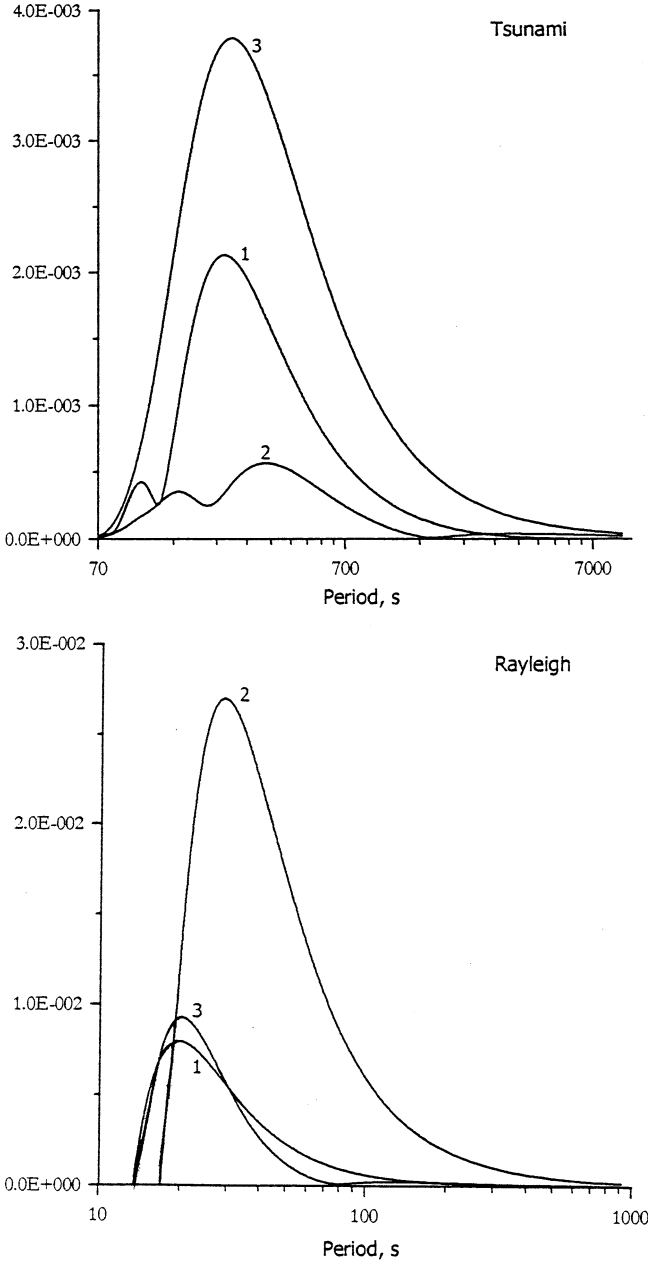

Figure 2
Tsunami and Rayleigh wave's normalized excitation functions for different source mechanisms.

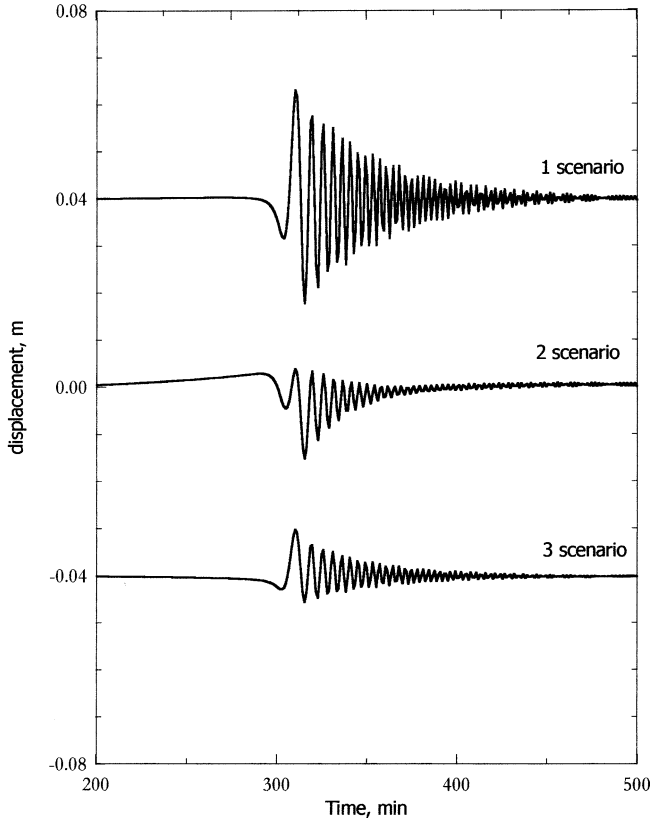

Figure 3
Comparison of theoretical marigrams of the tsunami wave at the 3588 km from distributed seismic sources with different geometries, located in hard sediments.

larger than that for a low dip fault (curve 2). Conversely, in the case of a Rayleigh wave the dip angle has the opposite effect. For a large dip angle (curves 1, 3) the amplitude of the excitation maximum is almost one order of magnitude smaller than for a low dip angle fault (curve 2).

Tsunami and Rayleigh synthetics for the above source scenarios at the distance of 3,588 km (propagation distance between PNG origin and Taiwan receiver) are given in Figures 3, and 4. The tsunami synthetics (Fig. 3) for the high angle dip-slip fault (curve 1) show wave amplitude twice as large as that for other source scenarios. In spite of the fact that the seismic moment of the aftershock event ($M_0 = 6.5 \times 10^{25}$ dyn-cm) is one order of magnitude smaller than that for the main event ($M_0 = 4.3 \times 10^{26}$ dyn-cm), the amplitude of the tsunami wave (curve 3) is comparable to that for the low angle reverse fault (curve 2). This is mainly due to the high dip angle ($\delta = 75°$) of this event.

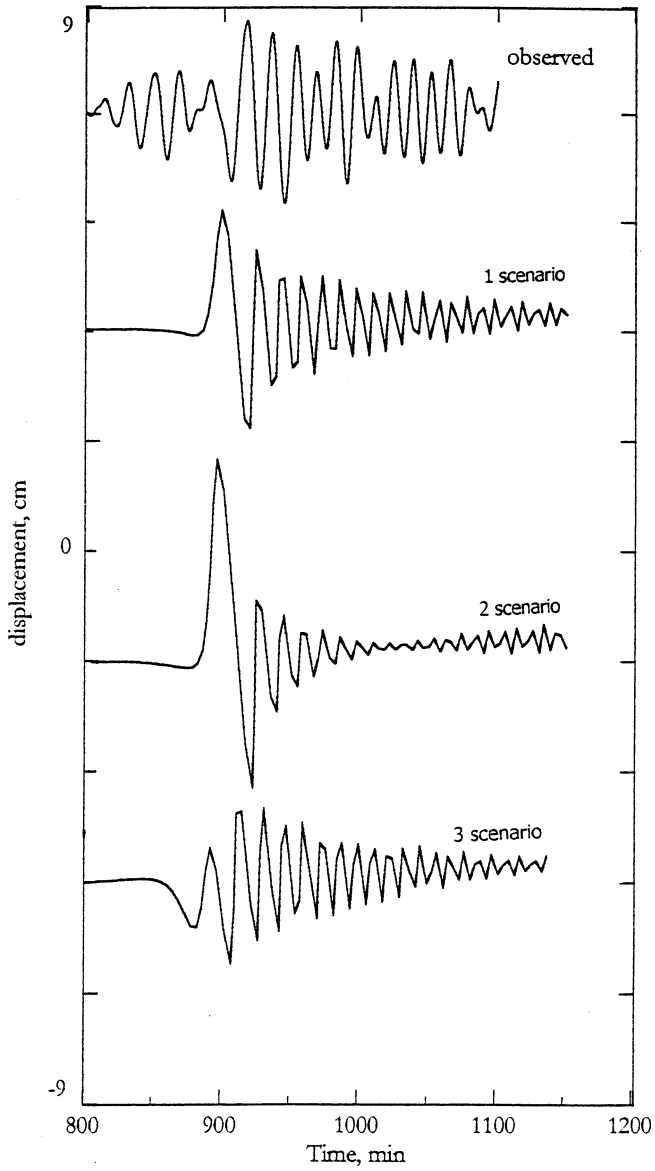

Figure 4
Comparison of observed (upper trace) and computed (low traces) seismograms of the Rayleigh wave at the 3588 km from distributed seismic sources with different geometries located in hard sediments. Curve 3 has been drawn 2 times its actual size.

The comparison of Rayleigh wave forms (RL) for the high-angle dip-slip fault (curve 1, Fig. 4) and for the low angle reverse fault (curve 2, Fig. 4) shows that wave amplitude for the second source scenario is almost two times higher then for the first

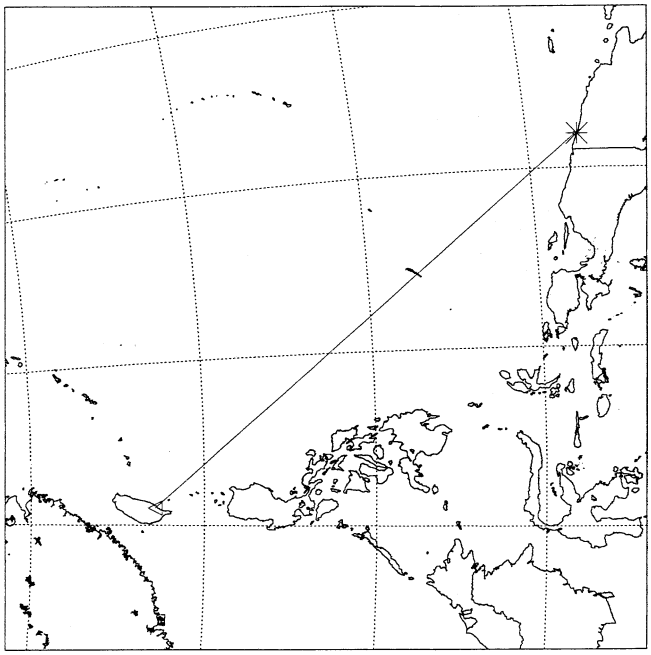

Figure 5
The location of the BATS station (triangle) used in this study. The map also shows the tsunami and Rayleigh waves computational area. A star represents the epicenter of the 1998 Papua New Guinea earthquake.

one. This behavior could be expected for the low dip angle events (YAMASHITA and SATO, 1976). For the aftershock event the amplitude of the Rayleigh wave (curve 3) decreases considerably because the seismic moment of this event ($M_0 = 6.5 \times 10^{25}$ dyn-cm.) is one order of magnitude smaller than that of the main shock ($M_0 = 4.3 \times 10^{26}$ dyn-cm), and also the high dip angle ($\delta = 75°$) makes an additional contribution to the dramatic decrease in the amplitude of the Rayleigh wave.

Comparing the observed Rayleigh form* with synthetics (curves 1, 2, 3), we conclude that both steep scenarios (main shock and aftershock) could be an explanation for the real record. It is reasonable since fault geometries of both steep shocks are quite similar except for a slight difference in the fault dip. However, the aftershock event was not energetic enough to excite tsunami wave. It will be clarified in the section below.

*Rayleigh waves were recorded at the station of Pacific site of Taiwan (Fig. 5), which belongs to the BATS instrumentation. All stations from this class are equipped with state-of-the-art very-broadband (Streckeisen STS-1 or STS-2) sensors and 24-bits digital recorders (Quanterra Q-680 Q-4120) (KAO *et al.*, 1998).

Energy Estimation Results

We first estimate energy E_{ts} (using expression (24)) for the case of a tsunami generated by a seismic source. For the low angle reverse fault scenario (second) the calculated tsunami energy was about 1.54×10^{20} erg. In the case of the high angle dip-slip fault (first scenario) the estimated energy was 9.9×10^{20} erg. These estimations are in good agreement with those obtained for tsunamigenic earthquakes of similar magnitude ($M = 7.0$): 1935 Sanriku ($E_{ts} = 0.4 \times 10^{21}$ erg), 1938 Ibaraki ($E_{ts} = 0.6 \times 10^{21}$ erg), 1938 Fukushima ($E_{ts} = 0.6 \times 10^{21}$ erg), 1938 Fukushima ($E_{ts} = 0.47 \times 10^{21}$ erg) (IIDA, 1963). However, the energy of tsunami wave ($E_{ts} \sim 10^{17}$ erg), excited by an aftershock event, is three orders of magnitude less than that produced by the earthquake with the geometry of the first scenario.

Then, on the basis of Rayleigh surface wave analysis, and using an analogous method (expression (24)), we calculate the dynamic energy released during the PNG earthquake. The estimated energy of the source with the first mechanism is 11.3×10^{21} erg, while that with the second mechanism is 2.56×10^{22} erg. Knowing these theoretically calculated energy values, we are able to estimate the E_z/E_{ts} ratio. For the first source scenario E_z/E_{ts} is 11.4 and in the case of the low angle fault E_z/E_{ts} is 170. Figure 6 (taken from IIDA, 1963) demonstrates the relationship between the ratio of seismic wave energy (E_z) to tsunami energy (E_{ts}) and the earthquake magnitude. Recognizing that the PNG earthquake magnitude is 7 we have plotted the data in this figure (marked by symbol **x**). Our energy estimates are clearly in good agreement with the results of IIDA (1963).

Taking into account the values of parameters α for interplate and intraplate events and calculating function $F(\delta, \lambda, h, r)$ according to (26), we estimate, using empirical relationship (27), the tsunami energy. It gives the order $\sim 10^{20}$ erg which is in good agreement with the theoretical estimation using formula (24).

On the basis of the results obtained from teleseismic analysis, KIKUCHI *et al.* (1999) have precluded the possibility of a slow earthquake in the case of the PNG event, however they have not excluded the possibility of an aseismic submarine landslide being the origin of a local massive tsunami. The intensity of a tsunami caused by this mechanism depends primarily on the relative scale of the phenomena, i.e., on the volume and density of the landslide, its depth of deposition, the slope angle of the sliding surface and the speed of the landslide movement. If assuming the tsunami source as a submarine slump with the parameters given in Table 3, we carry out an estimation of tsunami energy using the formulae introduced in Section 5b (expression (28)). According to our calculations, the value of tsunami energy is 0.38×10^{22} erg. We presented the lowest limit of the estimation of the seismic sea-wave energy for the case when only a small portion ($= 0.01$) of the slide energy transfers to tsunami energy. JIANG and LEBLOND (1992) have pointed out that the energy transfer ration can vary (from

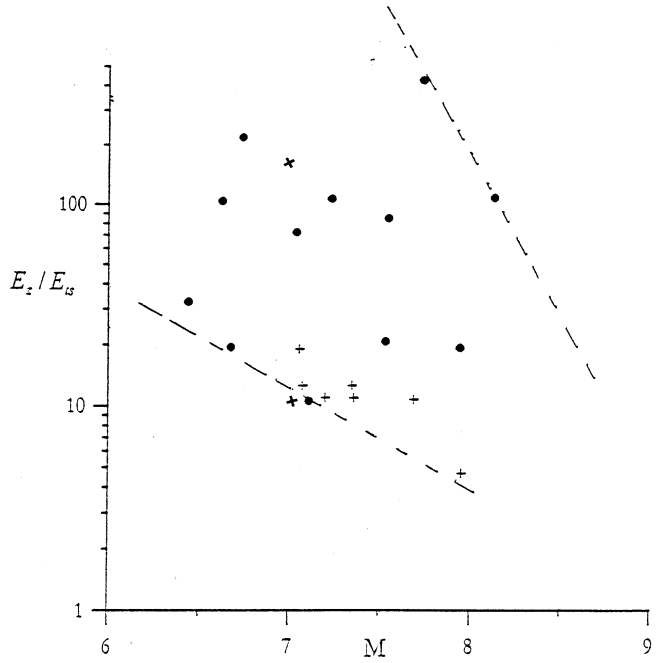

Figure 6

Relationship between the ratio of seismic wave energy to tsunami energy (E_z / E_{ts}) and the earthquake magnitude (M) (after IIDA, 1963); • — E_z / E_{ts} obtained by using tsunami period (Table 3 in IIDA, 1963); + — E_z / E_{ts} obtained by using magnitudes of tsunamis and earthquakes (Table 2 in IIDA, 1963); × — E_z / E_{ts} theoretically obtained values using the formula (24); - - - - - - (dashed lines) are ranges of E_z / E_{ts} against M (IIDA, 1963).

0.01 to 0.15) with time and mud properties. However, in spite of this, theoretically estimated energy is still slightly lower for a tsunami with the characteristic height of 15 m. There are well-known historical events of destructive tsunamis with amplitudes from 6 to 24 m and large energy: 1933 Sanriku (H = 24 m and $E_{ts} = 16 \times 10^{22}$ erg), 1944 Tonankai (H = 10 m and $E_{ts} = 16 \times 10^{22}$ erg), 1946 Nankaido-oki (H = 6 m and $E_{ts} = 16 \times 10^{22}$ erg), 1952 Tokachi (H = 5 m and $E_{ts} = 4 \times 10^{22}$ erg), 1952 Kamchatka (H = 18 m and $E_{ts} = 16 \times 10^{22}$ erg), etc. (IIADA *et al.*, 1967).

Table 3

Parameters for slide volume

Width of the slide (km)	3
Length of the slide (km)	5
Maximum thickness (m)	450
Slope (deg)	15

7. Conclusions

In this paper we have performed analytical modeling to study the excitation and far-field propagation of tsunami and Rayleigh waves from the 1998 PNG earthquake. Our numerical calculations for different source scenarios clearly show that far-field tsunami and Rayleigh waves are best explained by a high angle dip-slip source and agree with observations recorded in Taiwan and Japan (TANIOKA, 1999).

Assuming a seismic origin of the PNG tsunami, we calculate the tsunami energy. Theoretical estimates are in good agreement with those obtained empirically and yield the same order of $\sim 10^{21}$ erg for the energy value calculated by both methods. They are also in good agreement with historically known examples of tsunamigenic earthquakes of magnitude 7.

The calculation of the energy of slump generated tsunami yields the lowest limit of energy of the order of $\sim 10^{22}$ erg, which is one order of magnitude higher than in the case of fault-generated seismic sea waves but still low for a 15-m tsunami.

The results of our analytical modeling lead us to conclude that the far-field tsunami and Rayleigh waves are well explained by their seismic origin. Simply put, in the near-field zone the effects of both submarine slump and local bathymetry near the Sissano Lagoon must be included to obtain a good agreement between theory and observation.

Acknowledgments

This research was supported by a grant from the Institute of Earth Sciences of Academia Sinica, Taiwan. Constructive reviews of the manuscript by Dr. E. OKAL and one anonymous reviewer are gratefully acknowledged.

REFERENCES

ABE, K. (1979), *Size of Great Earthquakes of 1837–1974 Inferred from Tsunami Data*, J. Geophys. Res. *84*, 1561–1568.

AMBRASEYS, N. (1960), *The Seismic Sea Wave of July 9, 1956 in the Greek Archipelago*, J. Geophys. Res. *65*, 1257–1265.

BEN-MENAHEM, A. and HARKRIDER, D.B. (1964), *Radiation Patterns of Seismic Surface Waves from Buried Dipolar Point Sources in a Flat Stratified Earth*, J. Geophys. Res. *69*, 2605–2620.

BILEK, S. and LAY, T. (1999), *Rigidity Variations with Depth along Interplate Megathrust Faults in Subduction Zones*, Nature *400*, 443–446.

RINGDAL, F., MARSHALL, P.D., and ALEWINE, R.W. (1992), *Seismic Yield Determination of Soviet Underground Nuclear Explosions at the Shagan River Test Site*, Geophys. J. Int. *109*, 65–77.

DZIEWONSKI, A.M., EKSTROM, G., and MATERNOVSKAYA, N.N. (1999), *Centroid-moment Tensor Solution for July–September, 1998*, Phys. Earth Planet. Inter. *114*, 99–107.

EISSLER, H. and KANAMORI, H. (1987), *A Single-force Model for the 1975 Kalapana, Hawaii Earthquake*, J. Geophys. Res. *92*, 4827–4836.

GEIST, E. (2000), *Origin of the 17 July 1998 Papua New Guinea Tsunami: Earthquake or Landslide?* Seism. Res. Lett. *71*, 344–351.

GEIST, E. (2001), *Reply to Comment by E. A. Okal and C. E. Synolakis on "Origin of the 17 July 1998 Papua New Guinea Tsunami: Earthquake or Landslide?"* by E. L. Geist, Seism. Res. Lett. *72*, 367.

GUSIAKOV, V. (1975), *Excitation Tsunami and Ocean Rayleigh Waves by a Submarine Earthquake*, Math. probl. Geophys. 250–272.

HAMILTON, W. (1979), *Tectonics of the Indonesian Region*, U.S. Geol. Surv. Prof. Paper 1078, 354 pp.

HASEGAWA, H.S. and KANAMORI, H. (1987), *Source Mechanism of the Magnitude 7.2 Grand Banks Earthquake of November 18, 1929: Double-couple or Submarine Landslide?* Bull. Seismol. Soc. Am. *77*, 1984–2004.

HASKELL, N. (1953), *The Dispersion of Surface Waves on Multilayered Media*, Bull. Seismol. Soc. Am. *43*, 17–34.

HEINRICH, Ph., PIATANESI, A., and HEBERT, H. (2001), *Numerical Modeling of Tsunami Generation and Propagation from Submarine Slumps: The 1998 Papua New Guinea Event*, Geophys. J. Int. *145*, 97–111.

HOUSTON, H. (1999), *Slow Ruptures, Roaring Tsunamis*, Nature *400*, 409 pp.

IIDA, K. (1963), *A Relation of Earthquake Energy to Tsunami Energy and the Estimation of the Vertical Displacement in a Tsunami Source*, J. Earth. Sci. Nagoya Univ. *11*, 49–67.

IMAMURA, A. (1942), *History of Japanese Tsunamis*, Kaiyo-no Kagaku (Oceanography) *2* (in Japanese).

IWABUCHI, Y. *et al.* (2000), *Bathymetry of the Source Region of the 1998 Papua New Guinea Tsunami*, EOS. Trans. Am. Geophys. Un. *81*, 22 (abstract).

JIANG, L. and LEBLOND, P. (1992), *The Coupling of a Submarine Slide and the Surface Waves which it Generates*, J. Geophys. Res. *97*, C8, 12,731–12,744.

JOHNSON, J. and MOLNAR, P. (1972), *Focal Mechanisms and Plate Tectonics of the Southwest Pacific*, J. Geophys. Res. *77*, 5000–5032.

KAJUIRA (1981)

KANAMORI, H. (1972), *Mechanism of Tsunami Earthquakes*, Phys Earth Planet. Inter. *6*, 346–359.

KAO, H., JIAN, P.-R., MA, K.-F., HUANG, B.-S., and LIU, C.-C. (1998), *Moment-tensor Inversion for Offshore Earthquakes East of Taiwan and their Implications to Regional Collision*, Geophys. Res. Lett. *25*, 3619–3622.

KAWATA, Y. *et al.* (1999), *Tsunami in Papua New Guinea was as Intense as First Thought*, EOS, Trans. Am. Geophys. Un. *81*, 22 (abstract).

KEILIS-BOROK, V., *Seismic Surface Waves in a Laterally Inhomogeneous Earth* (Kluwer Academic Publishers, 1989).

KIKUCHI, M., YAMANAKA, Y., ABE, K., MORITA, Y. (1999), *Source Rupture Process of the Papua New Guinea Earthquake of July 17, 1998 Inferred from Teleseismic Body Waves*, Earth Planets and Space *51*, 1319–1324.

LEVSHIN, A.L. (1973), *Surface and Channel Seismic Waves*, Moscow, Nauka (in Russian).

MATSUYAMA, M., WALSH, J., and YEH, H. (1999), *The Effect of Bathymetry on Tsunami Characteristics at the Sissano Lagoon, Papua New Guinea*, Geophys. Res. Lett. *26*, 3513–3516.

MILOH, T. and STRIEM, H. (1978), *Tsunami Effects at Coast Sites due to Offshore Faulting*, Technophys. *46*, 347–356.

NEWMAN, A. and OKAL, E. (1998), *Teleseismic Estimates of Radiated Seismic Energy: The E/M_0 Discriminant for Tsunami Earthquakes*, J. Geophys. Res. *103*, 26,885–26,898.

NOVIKOVA, T., WEN, K-L., and HUANG, B.-S. (2002), *Analytical Model for Gravity and Rayleigh Wave Investigation in the Layered Ocean–Earth Structure*, Bull. Seismol. Soc. Am. 92, 723–738.

OKAL, E. and SYNOLAKIS, K. (2001), *Comment on "Origin of the 17 July 1998 Papua New Guinea Tsunami: Earthquake or Landslide?" by E. L. Geist*, Seism. Res. Lett. *72*, 363–367.

POD''YAPOL'SKY, G. S. (1968), *Excitation of a Long Gravitational Wave in the Ocean from a Seismic Source in the Crust*, Izv. AN SSSR, Fizika Zemli *1* (in Russian).

POD''YAPOL'SKY, G.S., *Generation of the Tsunami Wave by the Earthquake in Tsunamis in the Pacific Ocean*, pp. 19–32, (ed. Adams, W.M.), (East-West Center Press, Honolulu 1970).

PUNTODEWO, S., MCCAFFREY, R., CALAIS, E., BOCK, Y., RAIS, J., SUBARYA, R., POEWARIARDI, C., STEVENS, J., GENRICH, F., ZWICK, P., and WDOWINSKI, S. (1994), *GPS Measurements of Crustal Deformation within the Pacific-Australia Plate Boundary Zone in Iran Jaya, Indonesia*, Tectonophysics *237*, 141–153.

RIPPER, I. and LETZ, H. (1999), *The Sissano Lagoon (Aitape) Tsunami: Which Earthquake was Responsible?* Papua New Guinea Geological Survey, Port Moresby, 19 pp.

SATAKE, K. and TANIOKA, Y. (1999), *Source of Tsunami and Tsunamigenic Earthquakes in Subduction Zone*, Pure appl. geophys. *154*, 467–483.

SENO, T. and KAPLAN, D. (1988), *Seismotectonics of Western New Guinea*, J. Phys. Earth *36*, 107–124.

SOLOVIEV, S. and GO, C. (1974), *Catalogue of Tsunamis on the Western Coast of the Pacific Ocean (in Russian)*, Nauka, Moscow, 310 pp.

STRIEM, H. and MILOH, T. (1976), *Tsunami Induced by Submarine Slumpings off the Coast of Israel,* Int. Hydrographic Rev. *2*, 41–55.

SWEET, S. *et al*. (1999), *Seismic Reflection Images of the Source Region of the Papua New Guinea Tsunami of July 17, 1998*, EOS. Trans. Am. Geophys. Un. *80*, 46 (abstract).

SYNOLAKIS, C., BARDET, J.-P., BORRERO, J.C., DAVIES, H.L., OKAL, E., SILVER, E., SWEET, S. and TAPPIN, D. (2002), *The Slump Origin of the 1998 Papua New Guinea Tsunami*, Proc. R. Soc. London, A *458*, 763–789.

TAKAHASI, R. (1951), *An Estimate of Future Tsunami Damage along the Pacific Coast of Japan*, Bull. Earthq. Res. Inst. *29*, 71–95.

TANIOKA, Y. (1999), *Analysis of the Far-field Tsunamis Generated by the 1998 Papua New Guinea Earthquake*, Geophys. Res. Lett. *26*, 3393–3396.

TAPPIN, D., MATSUMOTO, T., WATTS, P., SATAKE, K., MCMURTY, G., MATSUYAMA, M., LOFOY, Y., TSUJI, Y., KANAMATSU, T., LUS, W., IWABUCHI, YO, YEH, H., MATSUMOTU, Y., NAKAMURA, M., MAHOI, M., HILL, P., CROOK, K., PATON, L., and WALSH, J. (1999), *Sediment Slump Likely Caused the 1998 Papua New Guinea Tsunami*, EOS. Trans. Am. Geophys. Un. *80*, 329, 334, 340.

TAPPIN, D. *et al*. (2000), *Submarine Slump Generation of the 1998 Papua New Guinea Tsunami: The Evidence so far*, EOS. Trans. Am. Geophys. Un. *80*, 46 (abstract).

THOMSON, W.T. (1950), *Transmission of Elastic Waves through a Stratified Solid Medium*, Jour. Appl. Phys. *21*, 89.

TREGONING, P., LAMBECK, K., STOLZ, A., MORGAN, P., MCCLUSKY, S., VAN DER BEEK, MCQUEEN, H., JACKSON, R., LITTLE, R., LAING, A., and MURPHY, B. (1998), *Estimation of Current Plate Motions in Papua New Guinea from Global Positioning System Observations*, J. Geophys. Res. *103*, 12,181–12,203.

YAMASHITA, T. and SATO, R. (1976), *Correlation of Tsunami and Suboceanic Rayleigh Wave Amplitudes. Possibility of the Use of Rayleigh Wave in Tsunami Warning System*, J. Phys. Earth *24*, 397–416.

(Received March 5, 2002; accepted September 26, 2004)